

RETRACTED ARTICLE: c(RGDyK)-decorated Pluronic micelles for enhanced doxorubicin and paclitaxel delivery to brain glioma

YuKun Huang¹
Wenchao Liu¹
Feng Gao¹
Xiaoling Fang²
Yanzuo Chen¹

¹Department of Pharmaceutics, School of Pharmacy, East China University of Science and Technology, ²Key Laboratory of Smart Drug Delivery, Ministry of Education & PLA, School of Pharmacy, Fudan University, Shanghai, People's Republic of China

Abstract: Brain glioma therapy is an important challenge in oncology. Here, doxorubicin (DOX) and paclitaxel (PTX)-loaded cyclic arginine-glycine-aspartic acid peptide (c(RGDyK))-decorated Pluronic micelles (cyclic arginine-glycine-aspartic acid-peptide-decorated Pluronic micelles loaded with doxorubicin and paclitaxel [RGD-PF-DP]) were designed as a potential targeted delivery system to enhance blood-brain barrier penetration and improve drug accumulation via integrin-mediated transcytosis/endocytosis and based on integrin overexpression in blood-brain barrier and glioma cells. The physicochemical characterization of RGD-PF-DP revealed a satisfactory size of 28.5 ± 0.12 nm with uniform distribution and core-shell structure. The transport rates across the in vitro blood-brain barrier model, cellular uptake, cytotoxicity, and apoptosis of U87 malignant glioblastoma cells of RGD-PF-DP were significantly greater than those of non-c(RGDyK)-decorated Pluronic micelles. In vivo fluorescence imaging demonstrated the specificity and efficacy of intracranial tumor accumulation of RGD-PF-DP. RGD-PF-DP displayed an extended median survival time of 39 days, with no serious body weight loss during the regimen. No acute toxicity to major organs was observed in mice receiving treatment doses of RGD-PF-DP by intravenous administration. In conclusion, RGD-PF-DP could be a promising vehicle for enhanced doxorubicin and paclitaxel delivery in patients with brain glioma.

Keywords: Pluronic micelles, integrin, blood-brain barrier, brain glioma, targeted delivery

Introduction

Approximately 80% of deadly tumors that develop in the central nervous system are malignant gliomas, which are essentially incurable.¹ Despite several treatment options, including surgical resection and radiation, tumor recurrence is common.² The median survival time of patients with glioblastoma multiforme, which is the most common and malignant subtype of glioma, is 12–18 months after diagnosis.³ This low median survival time is mostly attributed to the difficulties associated with treatment because of the blood-brain barrier (BBB) and blood-brain tumor barrier, which are major obstacles that prevent drugs from reaching the brain. In addition, factors such as the multidrug resistance of tumors, intracellular drug metabolism, and limited drug uptake contribute to the low median survival time of patients.⁴

Because of the compromised efficacy, it is important to deliver effective doses of therapeutic agents into the brain glioma sites. The effects of present chemotherapy are modest and often cause systemic side effects.^{5–8} The development of nanotechnology presents a promising approach for chemotherapeutics. Pluronic polymeric micelles, such as paclitaxel (PTX)-loaded vitamin E succinate-modified Pluronic micelles,⁹ gold nanoparticle crosslinked PF-PTX-micelles,¹⁰ 17-AAG-loaded Pluronic P-123, F-127

Correspondence: Yanzuo Chen
Department of Pharmaceutics, School of Pharmacy, East China University of Science and Technology, 130 Meilong Road, Xuhui, Shanghai 200237, People's Republic of China
Tel +86 21 6425 2449
Fax +86 21 6425 2449
Email chenyz@ecust.edu.cn

mixed micelles, and doxorubicin (DOX)-loaded Pluronic P-105, were recently introduced as treatments for glioma.^{11–13} However, their in vivo efficacy and therapeutic mechanism have not been illustrated in detail.

To overcome the BBB and blood–brain tumor barrier and deliver drugs to the central nervous system, strategies based on delivery systems that inhibit drug efflux transporters in the BBB have been proposed.¹⁴ Pluronic block copolymer nanoparticles enhance drug accumulation by inhibiting P-glycoprotein (P-gp) efflux, and their efficacy was demonstrated in the treatment of P-gp overexpressing tumors.¹⁵ Based on the inherent properties of Pluronic micelles, we aimed to develop a high efficiency brain glioma targeted delivery system. However, conventional Pluronic micelles, which target tumors via the enhanced penetration and retention effect, failed to accumulate in glioma tissues precisely. To solve this problem, Pluronic micelles decorated with specific ligands were developed to target cancer cells and increase intracellular delivery efficiency through specific receptor- or carrier-mediated endocytosis. Targeted polymeric micelle-based nanodelivery systems are efficient drug vehicles that have received increasing attention in recent years owing to their enhanced solubilization, small particle size, long circulation effect, selective targeting profile, altered drug internalization route, and subcellular localization properties. We selected cyclic Arg-Gly-Asp cyclic arginine-glycine-aspartic acid peptide (c(RGDyK)) as a candidate ligand because of its selective affinity for $\alpha_v\beta_3$ integrin, which is overexpressed in glioblastoma multiforme cells (eg, the U87 malignant glioblastoma [U87MG] cell line) and BBB cells (eg, the brain capillary endothelial cells [BCEC] cell line).¹⁶ We hypothesized that c(RGDyK)-decorated Pluronic micelles would be capable of overcoming the BBB, thus effectively accomplishing brain glioma targeting.

In previous studies, we developed c(RGDyK)-decorated Pluronic micelles loaded with DOX and PTX to form a dual-function drug delivery system (cyclic arginine-glycine-aspartic acid peptide-decorated Pluronic micelles loaded with doxorubicin and paclitaxel [RGD-PF-DP]) for antiangiogenesis and drug-resistant tumor treatment.¹⁷ c(RGDyK)-decorated Pluronic polymeric micelles were found to be a multidrug resistant tumor-sensitizer, as well as a dual-drug delivery carrier.¹⁸ Clinical studies have shown that combination treatment with DOX and PTX was more effective at increasing the rate of tumor regression than treatment with DOX or PTX as single agents.¹⁹ In the present study, we evaluated the efficacy of the delivery of c(RGDyK)-decorated Pluronic micelles in patients with brain glioma by measuring intracellular accumulation, cytotoxicity,

and cellular apoptosis in U87MG cells in vitro, and tumor-homing capability, anti-glioma efficacy, and safety evaluations in vivo.

Materials and methods

Materials and animals

DOX was obtained from Beijing Huafeng United Technology Co. Ltd. (Beijing, People's Republic of China) and PTX was purchased from Xi'an Sanjiang Bio-Engineering Co. Ltd. (Xi'an, People's Republic of China). Free PTX solution was prepared according to the commercial formulation of Taxol. c(RGDyK) (molecular weight = 619.51) was synthesized by the GL Biochem Ltd. (Shanghai, People's Republic of China). Pluronic micelles loaded with DOX and PTX (PF-DP) and c(RGDyK)-decorated PF-DP (RGD-PF-DP) were prepared in our lab through the method described previously.¹⁷ Dioctadecyl- ω ,3',3'-trimethylindotricarbocyanine iodide (DIR)-loaded Pluronic micelles (PF-DIR) and DIR-loaded c(RGDyK)-decorated Pluronic micelles (RGD-PF-DIR) were prepared as described before.^{20,21} 3-(4,5-Dimethyl-thiazol-2-yl)-2,5-diphenyl-tetrazolium bromide (MTT) and Hoechst 33342 were purchased from Sigma-Aldrich (St. Louis, MO, USA). Western blot related reagents were purchased from Beyotime Biotechnology Co. Ltd. (Nantong, People's Republic of China) and Santa Cruz Biotechnology (Dallas, TX, USA). Cell apoptosis analysis kits, Triton X-100, and BCA protein assay kit were purchased from Beyotime Biotechnology Co. Ltd. Annexin V-APC/7-AAD apoptosis detection kit was obtained from Nanjing KeyGen Biotechnology Co. Ltd. (Nanjing, People's Republic of China). Penicillin–streptomycin, Dulbecco's Modified Eagle's Medium (DMEM), Roswell Park Memorial Institute 1640 medium (RPMI-1640), fetal bovine serum (FBS), and 0.25% (w/v) trypsin solution were purchased from Gibco BRL (Thermo Fisher Scientific, Waltham, MA, USA). Purified deionized water was prepared by Milli-Q plus system (EMD Millipore Corporation, Billerica, MA, USA). All the other solvents were analytical grade.

The U87MG cell line was obtained from Shanghai Institute of Cell Biology. BCECs were kindly provided by Professor XG Jiang (School of Pharmacy, Fudan University). The human carcinoma KB cell line was purchased from Chinese Academy of Sciences Cells Bank (Shanghai, People's Republic of China). The use of these cell lines were carried out in accordance with the guidelines evaluated and approved by the ethics committee of East China University of Science and Technology. Culture plates and dishes were purchased from Corning Inc. (New York, NY, USA). KB cells were cultured in RPMI-1640, and U87MG cells and

BCECs were cultured in DMEM. Both media contained 10% FBS (Gibco BRL), 100 U/mL penicillin, and 100 µg/mL streptomycin at 37°C in a 5% CO₂ humidified environment incubator (Thermo Scientific, USA).

Male BALB/c nude mice (20±2) g, supplied by Department of Experimental Animals, Fudan University (Shanghai, People's Republic of China), were acclimated at 25°C and 55% of humidity under natural light/dark conditions for 1 week before the proposed experiments. All animal studies were carried out in accordance with guidelines evaluated and approved by the ethics committee of Fudan University. Mice that were unable to right themselves within 20 seconds were euthanized immediately. Animals were euthanized by CO₂ asphyxiation and death was confirmed by verifying respiratory arrest followed by cervical dislocation.

Characterization of c(RGDyK)-decorated Pluronic micelles

RGD-PF-DP was prepared as previously reported.¹⁷ The shape and morphology of RGD-PF-DP were studied by transmission electron microscopy (TEM) (Jeol JEM-1230; JEOL Ltd, Tokyo, Japan) and atomic force microscopy (Veeco Instruments Inc, Plainview, NY, USA). The particle size distribution and zeta potential of RGD-PF-DP were measured by the dynamic light scattering method using Malvern Autosizer 4700 (Malvern Instruments, Malvern, UK). DOX and PTX in RGD-PF-DP were extracted with acetonitrile and water (1:1, v/v) followed by high performance liquid chromatography determination and the drug loading coefficient was calculated.^{20,22}

Cellular uptake and competition assay

For the cellular uptake assay, U87MG and KB cells were seeded at a density of 1×10^5 cells/well in 24-well plates (Corning Costar, Tokyo, Japan) and examined under the microscope for confluency and morphology. When the confluency reached 80%, the medium was replaced with a mixture of DOX and PTX (DOX + PTX, DOX:PTX = 2:3, w/w), PF-DP, or RGD-PF-DP in FBS-free medium. After 2 hours of incubation at 37°C, the medium was removed, and cells were washed with cold phosphate-buffered saline (PBS, pH 7.4) twice and then lysed with 0.4 mL PBS containing 1% Triton X-100. After incubation, 100 µL of cell lysate was withdrawn and extracted with methanol (200 µL/sample), and then the mixture was exposed to probe-type ultrasonic treatment (400 W, 10 cycles with 2 seconds active – 3 seconds duration, JY92-II, Scientz Biotechnology Co., Ltd., Ningbo, People's Republic of China) in an ice bath. After extraction, the mixture was centrifuged at 6,000 rpm for 5 minutes, and

the supernatant was analyzed by high performance liquid chromatography. The protein content in the sample was determined using the BCA protein assay kit following the manufacturer's instructions. The cellular content of DOX and PTX was normalized to the total protein content.

A competition assay was performed to evaluate whether c(RGDyK) could hinder receptor-mediated endocytosis. U87MG and KB cells were preincubated with c(RGDyK) (0.3 µg/mL) for 1 hour, and the compound was removed before exposure to DOX + PTX, PF-DP, or RGD-PF-DP along with c(RGDyK) (each compound at a concentration of 0.3 µg/mL).

Antiproliferative activity against U87MG cells

U87MG cells in the logarithmic growth phase were seeded at a density of 2×10^4 cells/well. After 24 hours of culture at 37°C, the medium was removed, and the cells were incubated for 72 hours in medium containing DOX, PTX, DOX + PTX (DOX:PTX = 2:3, w/w), PF-DP, or RGD-PF-DP at various concentrations ranging from 0.001 to 1 µg/mL. Cell survival was determined using the tetrazolium salt MTT assay. Briefly, 100 µg of MTT reagent (in PBS, 20 µL/well) was added to the cells and cultured for another 4 hours. The supernatant was removed and replaced with dimethyl sulfoxide (200 µL/well), the plates were vigorously shaken, and the absorbance of each well was measured at 570 nm using a microplate reader (Safire 2, Tecan Group Ltd, Männedorf, Switzerland).^{5,23}

Cell apoptosis assay

Apoptosis was measured by assessing nuclear morphology in U87MG cells by Hoechst 33342 staining. Briefly, cells were seeded in a 6-well plate with a coverslip at a density of 1×10^5 cells/well and cultured for 24 hours. Cells were then incubated for another 24 hours in culture medium with or without DOX + PTX, PF-DP, or RGD-PF-DP (total drug concentration of 1 µg/mL). Samples were then fixed with 4% paraformaldehyde in PBS (pH 7.4) at room temperature for 15 minutes, stained for 15 minutes with 10 µg/mL Hoechst 33342 in PBS at room temperature, and washed twice with ice-cold PBS. Coverslips mounted onto glass slides were then examined under a fluorescent microscope (Leica DMI 4000B, Leica Microsystems, Wetzlar, Germany) as reported previously.^{5,17}

For the quantitative analysis of apoptosis, U87MG cells were seeded at a density of 5×10^5 cells/well in 6-well plates, incubated for 24 hours, and checked under the microscope for confluency and morphology. Cells were treated with or without DOX + PTX, PF-DP, and RGD-PF-DP (total drug

concentration of 1 $\mu\text{g/mL}$) for 24 hours. At the end of the treatment, cells were stained using the Annexin V-APC/7-AAD apoptosis detection kit according to the manufacturer's instructions. The stained cells were analyzed using a flow cytometer (FACSCalibur, BD Biosciences, San Jose, CA, USA).

Transport across the BCEC monolayer and competition assay

BCECs were seeded on polycarbonate 24-well Transwell membranes of 1.0 μm mean pore size and 0.33 cm^2 surface area (Becton Dickinson Labware, Franklin Lakes, NJ, USA) at a density of 5×10^4 cells/well. After 4 days, the cell monolayer integrity was monitored using an epithelial voltohmmeter (Millicell-RES, EMD Millipore Corporation, Billerica, MA, USA) to measure the transendothelial electrical resistance (TEER). Only cell monolayers with TEER values above 200 $\Omega \text{ cm}^2$ were selected for the experiment.⁵ The transport rate (%) was measured using DMEM as a transport medium. DOX, PF-DP, or RGD-PF-DP (5 $\mu\text{g/mL}$ DOX-equivalent) or PTX, PF-DP, or RGD-PF-DP (5 $\mu\text{g/mL}$ PTX-equivalent) was added into the donor chamber. Cells were incubated on a platform with shaking at 50 rpm at 37°C. A volume of 600 μL of sample medium was taken from the basolateral compartment at 2, 4, 8, and 24 hours, and replaced with an equal volume of fresh medium. The samples were freeze dried and examined by high performance liquid chromatography.

For the competition assay, the c(RGDyK) peptide was added to the donor chamber at a concentration of 0.3 $\mu\text{g/mL}$. After 1 hour of incubation at 37°C, the compounds were removed from the Transwell, and RGD-PF-DP along with c(RGDyK) peptide (the concentration of each compound was equal to 0.3 $\mu\text{g/mL}$) was added, followed by the above-mentioned steps. TEER was measured during the experiment to monitor the integrity of BCEC monolayers. In a parallel experiment, C-sucrose was added into the formulation solution to monitor the integrity of BCEC monolayers.

In vivo near-infrared optical imaging

In vivo fluorescence imaging analysis was used to evaluate the efficacy of glioma targeting of DIR-loaded c(RGDyK)-decorated Pluronic micelles. The intracranial U87MG glioblastoma model was established by inoculation of 5×10^5 U87MG cells (in 5 μL PBS) into the right striatum (1.8 mm lateral, 0.6 mm anterior to the bregma, and 3 mm of depth) of BALB/c nude mice by using a stereotactic fixation device with a mouse adaptor. The mice were intravenously injected

with 100 μL PF-DIR or RGD-PF-DIR (DIR content: 0.2%) 15 days postinoculation.²¹ Fluorescence scans were performed using the Maestro™ in vivo imaging system (excitation: 700–950 nm, emission: 780 nm long-pass; Cambridge Research and Instrumentation Inc, Woburn, MA, USA). The fluorescence scans were performed at 48 hours postadministration; tumor bearing mice were sacrificed and the glioma-bearing brain and major organs were excised. Organs were rinsed with PBS and fluorescence images acquired.

In vivo anti-glioma efficacy and safety evaluation

The in vivo anti-glioma efficacy and toxicity of RGD-PF-DP were evaluated in an intracranial U87MG glioma bearing mice model, which was established as described in “In vivo near-infrared optical imaging”. Three days after glioma inoculation (designated as day 0), the mice were randomly divided into four groups, and 0.1 mL of saline, DOX + PTX, PF-DP, or RGD-PF-DP (total drug concentration of 5 mg/kg) was injected via tail vein every 3 days for three continuous times. The body weight was monitored every other day and the death of mice was recorded. On day 18, four mice from each group were sacrificed and major organs (heart, liver, spleen, lung, and kidney) were harvested, fixed with paraformaldehyde for 48 hours, and embedded in paraffin. Blocks were cut into 5 μm sections, processed by routine hematoxylin and eosin staining, and visualized under microscope.

The brains were harvested in each group, and the activation of caspase was measured by Western blotting.²⁴ Glioma samples were homogenized with PBS containing protease inhibitors and total protein samples were resolved by 12% sodium dodecyl sulfate polyacrylamide gel electrophoresis. Proteins were transferred to polyvinylidene difluoride membranes, which were incubated with primary antibodies, followed by horseradish peroxidase-conjugated secondary antibodies and treatment with 3,3'-diaminobenzidine and H_2O_2 . Images were captured using the Tanon GIS-2008 (Tanon Science & Technology Co., Shanghai, People's Republic of China).

The other eight mice in each group were used for monitoring survival curves using the Kaplan–Meier method, and the median survival was calculated with GraphPad Prism v5.0 (GraphPad Software Inc., La Jolla, CA, USA).

Data analysis

Data were expressed as mean \pm standard deviation. Two tailed *t*-test for two groups and two tailed multiple comparisons were performed using ANOVA followed by post hoc tests. Survival was analyzed using the Kaplan–Meier method

and log-rank test. A value of $P < 0.05$ was considered to be significant.

Results and discussion

Characterization of c(RGDyK)-decorated Pluronic micelles

The mean diameter of RGD-PF-DP was 28.5 ± 0.12 nm with an acceptably good polydispersity index (< 0.15) (Figure 1A) and a spherical shape, as determined by TEM (Figure 1B). Micelles smaller than 200 nm may benefit from the increased permeability of the tumor vasculature, which is known as the enhanced permeability and retention effect of tumors.^{25,26} As shown in the TEM image, a clear peptide-engineered poly-oxyethylene corona was observed on the micelle surface. The particle size in the atomic force microscopy images was in good correspondence with that measured by the laser scattering technique and TEM (Figure 1C). The zeta potential

of RGD-PF-DP was close to neutral (within ± 5 mV), which may lead to a tendency toward the aggregation of micelles. The DOX and PTX loading coefficients of RGD-PF-DP were $1.01\% \pm 0.15\%$ and $1.54\% \pm 0.24\%$, respectively. These results demonstrated that RGD-PF-DP have an acceptable drug loading capability.

Cellular uptake and competition assay

To evaluate the effect of the $\alpha_v\beta_3$ integrin receptor on the cellular uptake of RGD-PF-DP, U87MG cells were selected as high $\alpha_v\beta_3$ integrin receptor expressing cells, whereas KB cells were used as the $\alpha_v\beta_3$ integrin receptor-deficient cell model.²⁷ As shown in Figures 2A and B, the intracellular DOX and PTX levels were higher in the RGD-PF-DP group than in the PF-DP and DOX + PTX groups in U87MG cells ($P < 0.01$), suggesting that c(RGDyK) decoration on the Pluronic micelle surface significantly facilitated the uptake

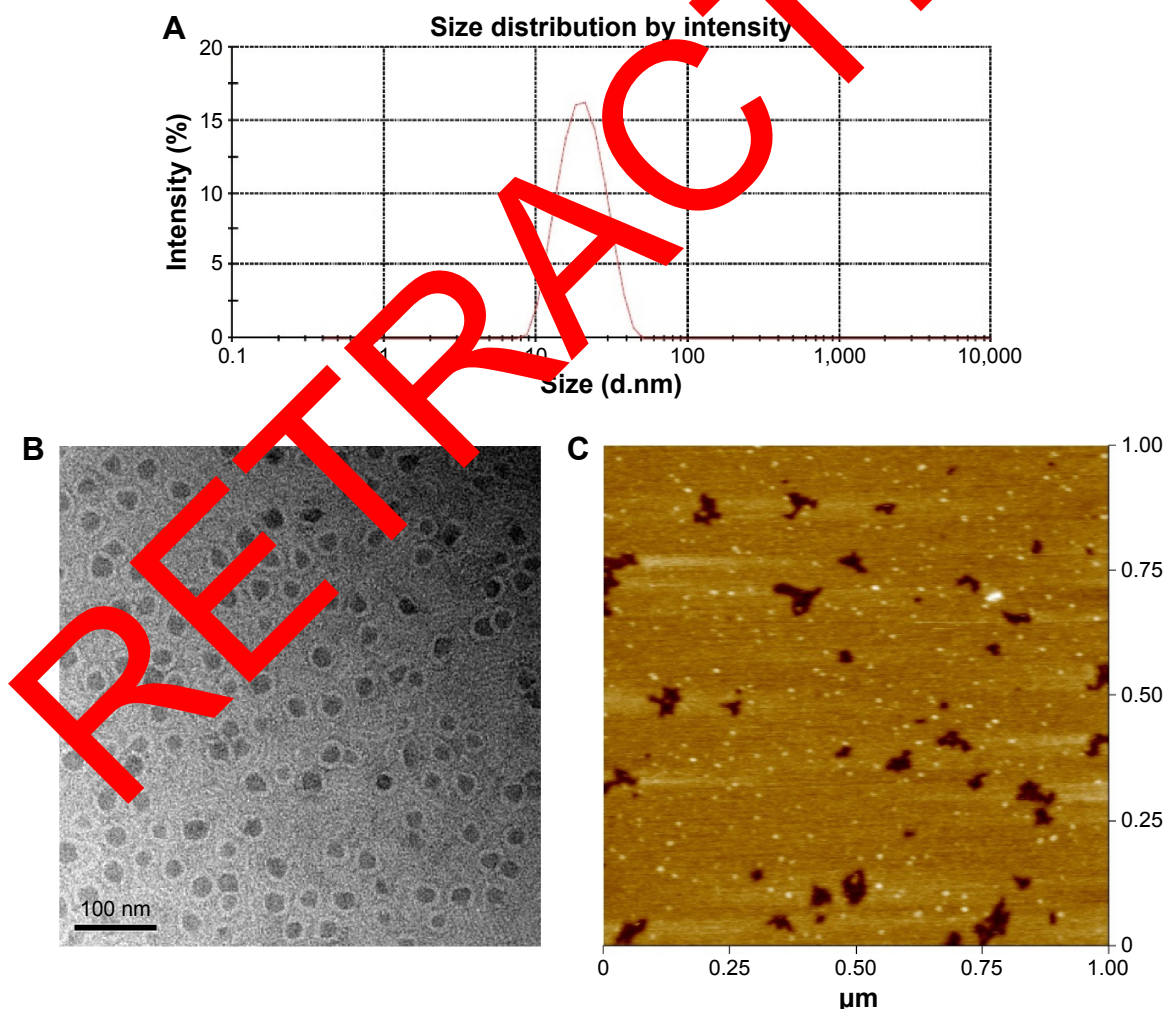


Figure 1 The characterization of RGD-PF-DP micelles.

Notes: Particle size and size distribution of RGD-PF-DP measured by dynamic light scattering (A). Transmission electron microscopy image of RGD-PF-DP (B). Atomic force microscopy image of RGD-PF-DP (C).

Abbreviation: RGD-PF-DP, cyclic arginine-glycine-aspartic acid peptide-decorated Pluronic micelles loaded with doxorubicin and paclitaxel.

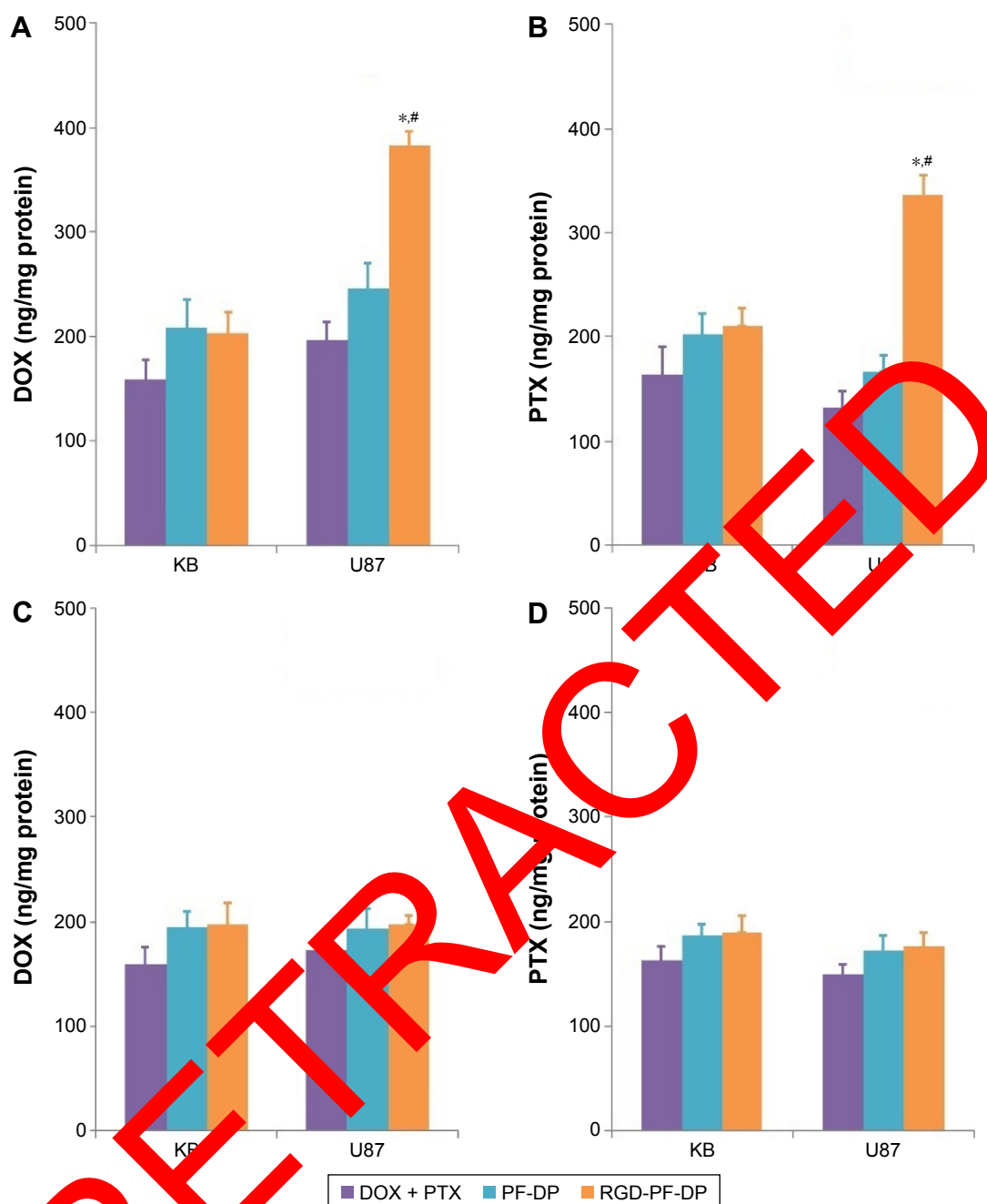


Figure 2 Cellular uptake in U87MG and KB cells.

Notes: U87MG and KB cellular uptake after 2-hour treatment with DOX + PTX, PF-DP, or RGD-PF-DP (1 μ g/mL DOX-equivalent) (A) and DOX + PTX, PF-DP, or RGD-PF-DP (1 μ g/mL PTX-equivalent) (B) at 37°C. 1-hour preincubation with 0.3 μ g/mL of free c(RGDyK) and then exposure to DOX + PTX, PF-DP, or RGD-PF-DP (1 μ g/mL DOX-equivalent) (C) and DOX + PTX, PF-DP, or RGD-PF-DP (1 μ g/mL PTX-equivalent) (D). Mean \pm standard deviation (n=3). * P <0.01, compared with DOX + PTX treatment; # P <0.01, compared with PF-DP treatment.

Abbreviations: DOX + PTX, physical mixture of doxorubicin and paclitaxel in weight ratio of 2:3; PF-DP, Pluronic micelles loaded with doxorubicin and paclitaxel; RGD-PF-DP, cyclic arginine-glycine-aspartic acid peptide-decorated Pluronic micelles loaded with doxorubicin and paclitaxel; DOX, doxorubicin; PTX, paclitaxel; U87MG, U87 malignant glioblastoma; KB, human nasopharyngeal carcinoma.

of DOX and PTX by U87MG cells.²⁸ Addition of free c(RGDyK) (Figure 2C and D) did not increase the cellular uptake in the RGD-PF-DP group compared with that of the PF-DP or DOX + PTX group in U87MG cells (P >0.05). The results demonstrated that the enhanced cellular uptake

of RGD-PF-DP may be attributed to the c(RGDyK) active targeting since the $\alpha_v\beta_3$ integrin receptor is overexpressed in U87MG cells. By contrast, both PF-DP and RGD-PF-DP showed the same cellular uptake as DOX + PTX in KB cells, regardless of whether free c(RGDyK) was added or not

($P>0.05$), supporting that the cellular uptake of RGD-PF-DP was mainly mediated by the interaction between c(RGDyK) and integrin proteins.

Antiproliferative activity against U87MG cells

The antiproliferative effect of DOX + PTX, PF-DP, and RGD-PF-DP on U87MG cells was evaluated using the MTT assay. The results showed that Pluronic micelles reduced cell viability compared with the effect of free drug (Figure 3). At various concentrations, RGD-PF-DP exhibited the strongest inhibitory effect on the proliferation of U87MG cells among free drugs and PF-DP. The IC_{50} values of DOX, PTX, DOX + PTX, PF-DP, and RGD-PF-DP were 0.067 ± 0.011 , 0.061 ± 0.005 , 0.041 ± 0.006 , 0.032 ± 0.001 , and 0.020 ± 0.007 $\mu\text{g/mL}$, respectively. The cytotoxicity of RGD-PF-DP was significantly higher than that of the other four groups ($P<0.01$), which was consistent with the cellular uptake results. RGD-PF-DP significantly enhanced the uptake of DOX and PTX by U87MG cells, leading to a higher cytotoxicity. The c(RGDyK) peptide facilitated RGD-PF-DP integrin protein-rich U87MG cellular uptake, resulting in increased intracellular drug concentration,²⁹ which might improve the antiproliferative activity of RGD-PF-DP.

Cell apoptosis assay

U87MG nuclear staining was performed to qualitatively observe cell apoptosis after different treatment in this study.

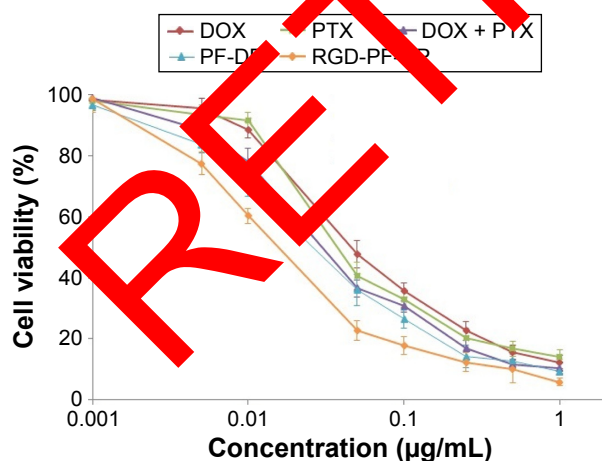


Figure 3 In vitro cytotoxicity of various formulations against U87MG cells at 72 hours.

Note: Mean \pm standard deviation ($n=3$).

Abbreviations: DOX, doxorubicin; PTX, paclitaxel; DOX + PTX, physical mixture of doxorubicin and paclitaxel in weight ratio of 2:3; PF-DP, Pluronic micelles loaded with doxorubicin and paclitaxel; RGD-PF-DP, cyclic arginine-glycine-aspartic acid peptide-decorated Pluronic micelles loaded with doxorubicin and paclitaxel; U87MG, U87 malignant glioblastoma.

The nuclei of untreated U87MG cells showed homogeneous fluorescence with no evidence of segmentation and fragmentation after Hoechst 33342 staining (Figure 4A). By contrast, nuclei became fragmented when the cells were treated with different formulations for 24 hours, showing segmentation into dense nuclear fractions and distribution into apoptotic bodies. RGD-PF-DP induced more severe fragmentation of the cell nuclei than DOX + PTX or PF-DP.

For quantitative analysis, the Annexin V-APC/7-ADD apoptosis detection kit was used to stain the cells, and the rate of cell apoptosis was determined by flow cytometry as shown in Figure 4B. The percentages of late and total apoptosis in the control group were $2.35\pm0.35\%$ and $4.79\pm0.32\%$, respectively, showing the lowest apoptosis rates among the four treatment groups. The rates of late and total apoptosis were $13.01\pm4.11\%$ and $73.38\pm3.48\%$, respectively, in the DOX + PTX group; $16.79\pm1.32\%$ and $83.39\pm2.61\%$, respectively, in the PF-DP group ($P<0.05$); and $35.25\pm2.61\%$ and $87.03\pm2.13\%$, respectively, in the RGD-PF-DP group ($P<0.01$). This was consistent with the in vitro cytotoxicity results and suggested that RGD-PF-DP induced more late apoptosis, possibly due to enhanced integrin receptor-mediated cellular uptake, and resulted in a higher cytotoxicity than PF-DP.

Transport across the BCEC monolayer and competition assay

The transport rates across the BCEC monolayer in vitro over a period of 24 hours are shown in Figure 5A. The transport rate of DOX in BCECs was significantly higher in both micelle groups than in the free drug group ($P<0.05$) during the experimental period, which could be attributed to the P-gp inhibiting property of Pluronic block polymers, and the results were consistent with those of our previous studies.^{18,20} The transport rate of DOX at 24 hours was $11.70\pm0.41\%$ for PF-DP and $20.45\pm1.27\%$ for RGD-PF-DP, which indicated that the transport of DOX across the BCEC monolayer was significantly increased when PF-DP was coupled with c(RGDyK) ($P<0.01$).³⁰ In the competition assay, the c(RGDyK) peptide was added in advance. In the presence of free c(RGDyK) peptide, the transport of RGD-PF-DP was dramatically reduced ($P<0.05$) because of the competitive binding of free c(RGDyK) peptide to integrin $\alpha_v\beta_3$ on BCECs. This indicated that the transport of RGD-PF-DP across the BBB could be significantly increased by integrin $\alpha_v\beta_3$ receptor-mediated endocytosis as a result of the expression of integrin $\alpha_v\beta_3$ on BCECs.³¹ Suppression of P-gp efflux and targeting of c(RGDyK) enabled drugs to cross

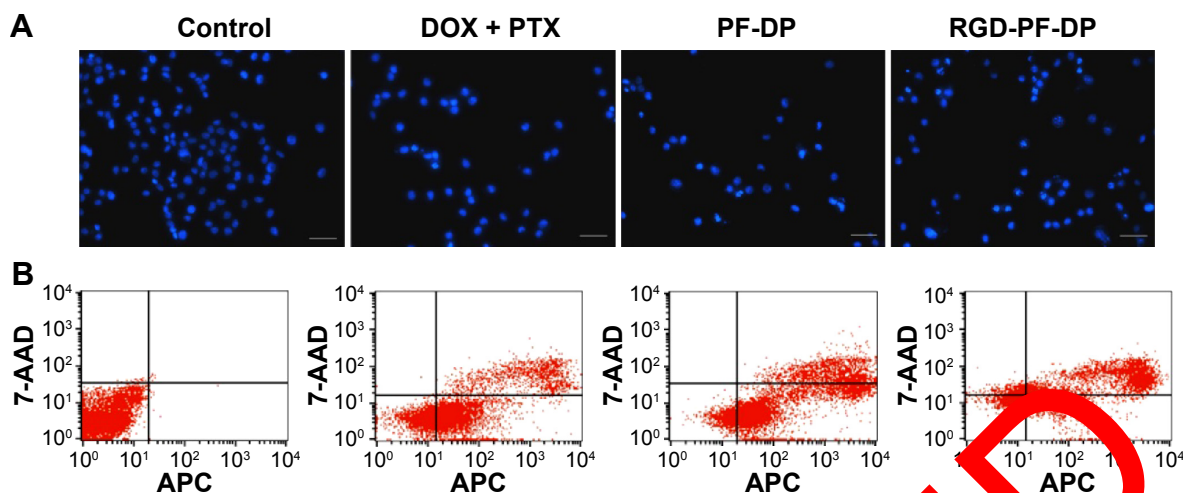


Figure 4 Cell apoptosis in U87MG cells after treatment with various formulations for 24 hours at equivalent total drug concentrations (1 $\mu\text{g}/\text{mL}$). **Notes:** Fluorescence micrographs of U87MG cell nuclei labeled by Hoechst 33342 (A). Flow cytometric analysis of cell apoptosis after treatment (normal U87MG cells without any treatment served as the control). Bar = 50 μm .

Abbreviations: DOX + PTX, physical mixture of doxorubicin and paclitaxel in weight ratio of 2:3; PF-DP, Pluronic micelles loaded with doxorubicin and paclitaxel; RGD-PF-DP, cyclic arginine-glycine-aspartic acid peptide-decorated Pluronic micelles loaded with doxorubicin and paclitaxel; U87MG, U87 malignant glioblastoma.

the BBB, thus increasing drug concentration in the glioma area and reducing side effects. The transport rate of PTX in BCECs was comparable to that of DOX (Figure 5B). PF-DP and RGD-PF-DP transport across the BCEC monolayer was time-dependent when the incubation time ranged from 2 to 24 hours. The transport rate of free DOX was <1% and transport was time-independent. This could be ascribed to the hydrophilicity of DOX as well as the efflux pumping effect of BCECs.

The integrity of the BCEC monolayer *in vitro* was monitored by TEER and the permeability of ^{14}C -sucrose during the experiment. The TEER value of the BCEC monolayer remained higher than 200 $\Omega \cdot \text{cm}^2$ and the permeability

of ^{14}C -sucrose was not significantly different from that of the control.

In vivo near-infrared imaging

In vivo multispectral fluorescence imaging analysis was performed to evaluate the potential targeting effect of RGD-PF-DP in subcutaneous tumor-bearing nude mice based on the fluorescence of DIR. After administration via tail vein, the biodistribution of micelles was observed using noninvasive near-infrared fluorescence imaging in live animals. Compared with the PF-DIR group, the fluorescence signal in the tumor-bearing brain of the RGD-PF-DIR group was stronger at 48 hours postinjection as shown in Figure 6A,

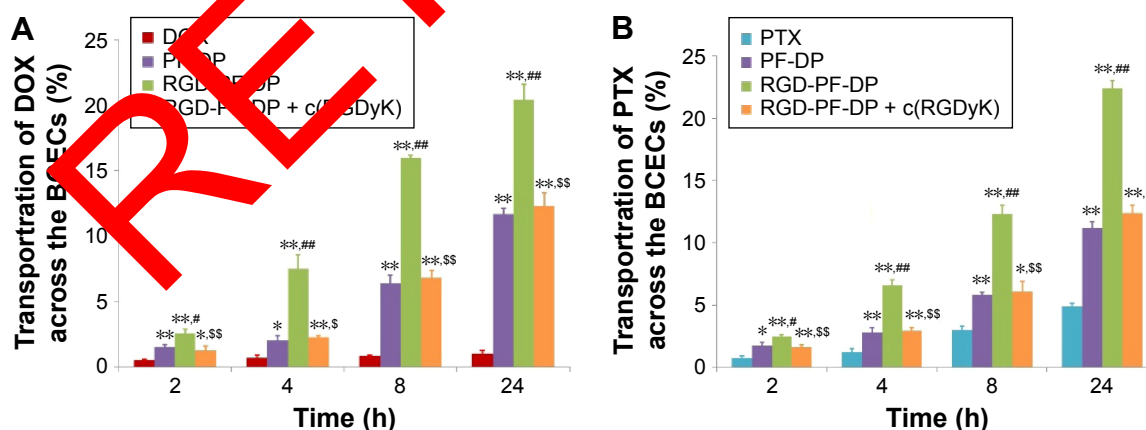


Figure 5 Transport rates of DOX and PTX across the BCEC *in vitro* during 24 hours.

Notes: Mean \pm standard deviation ($n=3$). * $P<0.05$, ** $P<0.01$, compared with DOX (A) or PTX (B) treatment. ## $P<0.05$, ### $P<0.01$, compared with PF-DP treatment; \$ $P<0.05$, \$\$ $P<0.01$, compared with RGD-PF-DP treatment.

Abbreviations: DOX, doxorubicin; PTX, paclitaxel; BCECs, brain capillary endothelial cells; PF-DP, Pluronic micelles loaded with doxorubicin and paclitaxel; RGD-PF-DP, cyclic arginine-glycine-aspartic acid peptide-decorated Pluronic micelles loaded with doxorubicin and paclitaxel; c(RGDyK), cyclic arginine-glycine-aspartic acid peptide; h, hours.

suggesting that decoration with the c(RGDyK) peptide enhanced the accumulation of micelles in brain tissues.

The results of ex vivo evaluation of excised organs (heart, liver, spleen, lung, and kidney) and the glioma-bearing brain at 48 hours postinjection are shown in Figure 6B. Micelles accumulated in the glioma-bearing brain in both groups. Organ imaging was used to calculate the mean fluorescence intensities of tumor, brain, liver, spleen, lung, kidney, and heart (Figure 6C). Quantitative analysis of the biodistribution of RGD-PF-DIR and PF-DIR in tumor-bearing mice revealed that the fluorescence intensity was higher in tumors treated with RGD-PF-DIR than in those treated with PF-DIR ($P<0.01$). The higher distribution of RGD-PF-DIR in tumor-bearing brains indicated that modification with c(RGDyK) enhanced the accumulation of micelles in tumors. Accumulation of RGD-PF-DIR in the heart, liver, and spleen was lower than that of PF-DIR ($P<0.05$). These results indicated that RGD-PF-DIR could substantially home to integrin-rich tumors in vivo and decrease the nonspecific uptake of the reticuloendothelial systems.

In vivo anti-glioma efficacy

The anti-glioma effect of RGD-PF-DP was compared with those of saline, DOX + PTX, and PF-DP by calculating the

the survival time of intracranial glioma-bearing mice. Figure 7A shows the Kaplan–Meier survival curves. As shown in Table 1, the median survival time of mice treated with RGD-PF-DP (39 days) was significantly longer than those of mice treated with saline (23 days, $P<0.01$), DOX + PTX (23 days, $P<0.01$), and PF-DP (31 days, $P<0.05$) according to the log-rank analysis. Glioma is divided into two grades based on pathology. In low-grade glioma, the BBB is intact and the drug delivery system should be able to cross the BBB and target the glioma.³² However, in advanced-grade glioma, the BBB is disrupted by impaired capillary endothelial tight junctions. The survival time of intracranial U87MG glioma-bearing mice was assessed in low- and advanced-grade glioma. At the low-grade stage, the significant suppression of glioma growth in the RGD-PF-DP group could be explained by the P-gp inhibiting property of Pluronic block polymers and integrin $\alpha_v\beta_3$ receptor-mediated endocytosis, which facilitated the transport of RGD-PF-DP across the BBB. At the advanced-grade stage, the BBB was destroyed to some extent as a result of tumor progression,^{33,34} and the increased local concentration of RGD-PF-DP in the tumor could be attributed to passive targeting and integrin receptor-mediated cellular uptake. In addition, considering the neovasculature targeting ability

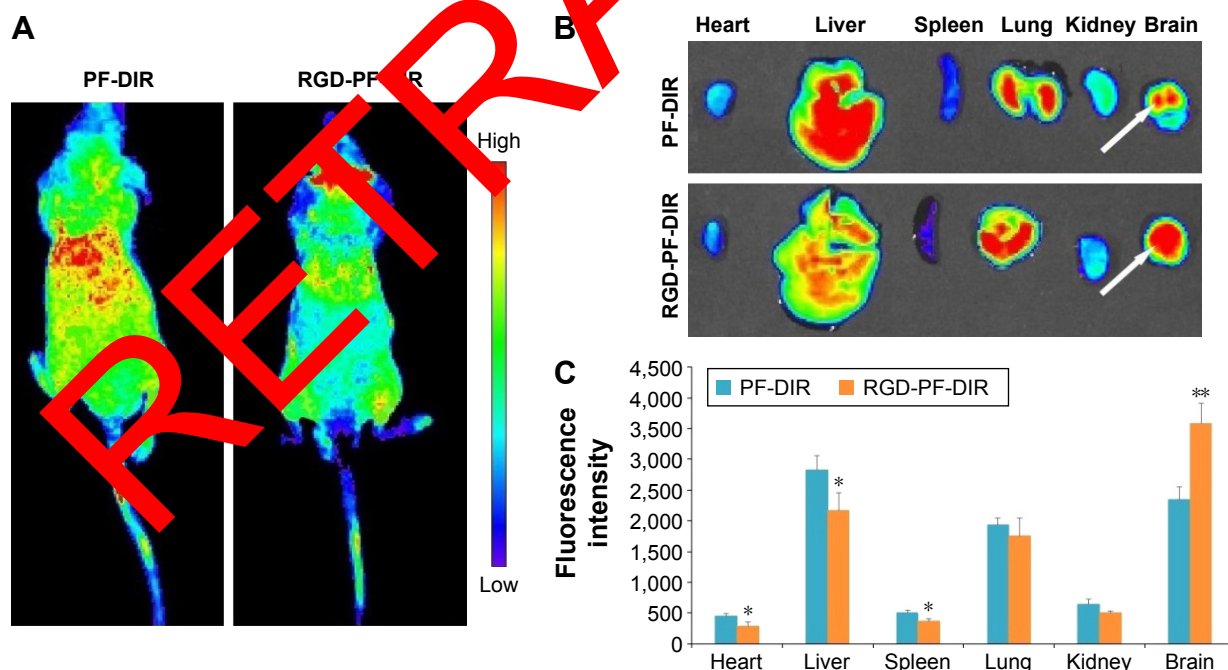


Figure 6 In vivo fluorescence imaging of intracranial U87MG glioma tumor-bearing nude mice 48 hours after intravenous injection of PF-DIR or RGD-PF-DIR (A); representative ex vivo near-infrared fluorescence images of dissected organs of intracranial U87MG glioma tumor-bearing nude mice sacrificed at 48 hours after intravenous injection of PF-DIR or RGD-PF-DIR (B); fluorescence intensity of PF-DIR and RGD-PF-DIR in various organs (C).

Notes: Mean \pm standard deviation ($n=3$). The tumor location is specified with a white arrow. * $P<0.05$, ** $P<0.01$, compared with the PF-DIR group.

Abbreviations: PF-DIR, dioctadecyl-3,3',3'-tetramethylindotricarbocyanine iodide-loaded Pluronic micelles; RGD-PF-DIR, dioctadecyl-3,3',3'-tetramethylindotricarbocyanine iodide-loaded cyclic arginine-glycine-aspartic acid peptide-decorated Pluronic micelles; U87MG, U87 malignant glioblastoma.

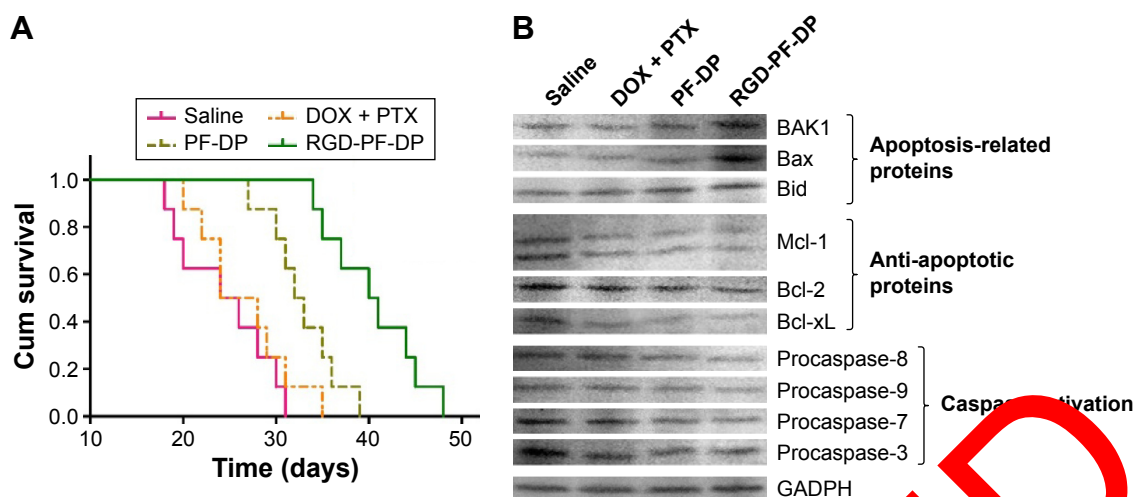


Figure 7 Kaplan–Meier survival curves and Western blot analysis.

Notes: Kaplan–Meier survival curves of intracranial U87MG glioma tumor-bearing nude mice (**A**). Effects of RGD-PF-DP on apoptosis-related proteins, anti-apoptotic proteins, and caspase activation by Western blot analysis (**B**).

Abbreviations: DOX + PTX, physical mixture of doxorubicin and paclitaxel in weight ratio of 2:3; PF-DP, Pluronic micelles loaded with doxorubicin and paclitaxel; RGD-PF-DP, cyclic arginine-glycine-aspartic acid peptide-decorated Pluronic micelles loaded with doxorubicin and paclitaxel; GADPH, glyceraldehyde-3-phosphate dehydrogenase; U87MG, U87 malignant glioblastoma.

of RGD, the better anti-glioma efficacy in RGD-PF-DP treatment group could be partially attributed to the enhanced accumulation in the neovasculature of brain tumor. Both DOX and PTX are commonly used anticancer drugs, and their efficacy is related to their capacity to induce cancer cells apoptosis.³⁵ We therefore analyzed the effect of RGD-PF-DP on apoptosis by Western blotting using tumor tissues excised from animals (Figure 7B). The apoptotic process in cancer cells is largely governed by interactions of proteins in the Bcl-2 family, which is divided into two functionally distinct groups.³⁶ Proteins in the first group, such as BAK1, Bax, and Bid promote apoptosis, whereas proteins in the second group, including Bcl-2, Bcl-xL, and Mcl-1, inhibit apoptosis. RGD-PF-DP upregulated apoptosis-related proteins including BAK1, Bax, and Bid, compared with the effects of DOX + PTX and PF-DP. The expression of anti-apoptotic proteins, such as Bcl-2, Bcl-xL, and Mcl-1, was lower in RGD-PF-DP group than in the other three groups.

Caspase activation plays a central role in the execution of apoptosis and active caspases cleave many important intracellular substrates, leading to the characteristic morphological changes associated with apoptotic cells.³⁷ Here, caspase activation was determined by measuring the levels of procaspase-3, -7, -8, and -9 in tumor tissues. Treatment with RGD-PF-DP downregulated procaspase-3, -7, -8, and -9 indicating that more precursor forms were cleaved into active subunits. Taken together, these results indicated that RGD-PF-DP induced tumor cell apoptosis via various pathways, thus enhancing the therapeutic efficacy of DOX and PTX in brain glioma.

In vivo safety evaluation

The toxicity of RGD-PF-DP for application in biomedicine is of concern. We therefore evaluated the systemic toxicity of RGD-PF-DP in intracranial U87MG glioma-bearing BALB/c mice after intravenous injection of RGD-PF-DP (dose of 5 mg/kg) three times every 3 days. Changes in body weight

Table 1 In vivo anti-glioma effects of dual-drug-loaded formulations on intracranial U87MG glioma-bearing mice model

Groups	Dose (mg/kg)	MST (days)	Median survival time (days)	Compared with		
				Saline	DOX + PTX	PF-DP
Saline	–	24.5±1.79	24	–	–	–
DOX + PTX	5	26.6±1.77	24	P=0.408	–	–
PF-DP	5	32.8±1.33	32	P=0.002	P=0.028	–
RGD-PF-DP	5	40.5±1.76	40	P=0.00004	P=0.0002	P=0.003

Note: Values are mean ± standard deviation (n=8).

Abbreviations: U87, malignant glioblastoma; MST, mean survival time; DOX + PTX, physical mixture of doxorubicin and paclitaxel in weight ratio of 2:3; PF-DP, Pluronic micelles loaded with doxorubicin and paclitaxel; RGD-PF-DP, cyclic arginine-glycine-aspartic acid peptide-decorated Pluronic micelles loaded with doxorubicin and paclitaxel.

were monitored as a marker of overall toxicity after 18 days because the mice in the physiological saline group died on day 18 after implantation. The DOX + PTX group showed a greater weight loss than the saline group, which could be due to the cardiotoxicity of DOX. Mice in the RGD-PF-DP group

showed a lower body weight loss than mice in the other three groups at the same time points (Figure 8A). These results implied that RGD-PF-DP was a safe and effective drug delivery system for U87MG glioblastoma treatment. In addition, there were no obvious histopathological abnormalities

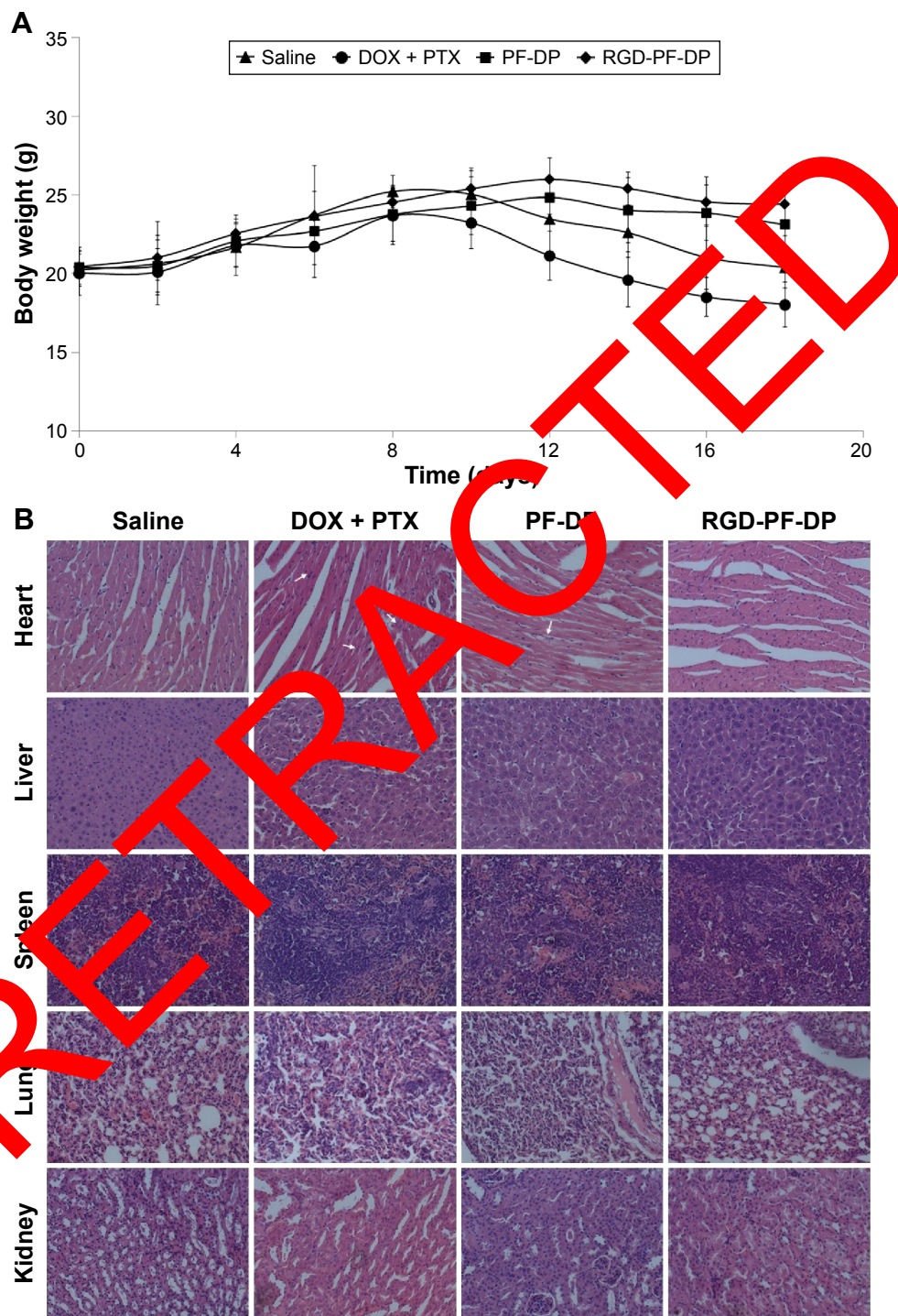


Figure 8 Changes in body weight of tumor-bearing nude mice and histochemistry analysis.

Notes: Changes in body weight of intracranial U87MG glioma tumor-bearing nude mice as a function of time (A). Histochemistry analysis of the heart, liver, spleen, lung, and kidney sections stained with hematoxylin and eosin after treatment with different formulations (B). Mean \pm standard deviation (n=12). Original magnification: $\times 20$. The white arrows indicate the position of the apoptotic nuclei.

Abbreviations: DOX + PTX, physical mixture of doxorubicin and paclitaxel in weight ratio of 2:3; PF-DP, Pluronic micelles loaded with doxorubicin and paclitaxel; RGD-PF-DP, cyclic arginine-glycine-aspartic acid peptide-decorated Pluronic micelles loaded with doxorubicin and paclitaxel; U87MG, U87 malignant glioblastoma.

or lesions in organs, such as the heart, liver, spleen, lung, and kidney in the RGD-PF-DP group, suggesting that RGD-PF-DP did not cause an inflammatory response, as shown in Figure 8B. However, cardiac tissue degeneration, necrosis, and heart congestion were observed in the DOX + PTX group, and daily injections of DOX caused weight loss and cardiotoxicity.³⁸ These results suggested that the cardiotoxicity of DOX is attenuated when the drug is delivered by a Pluronic micelle nanocarrier, which could be attributed to the modified DOX biodistribution conferred by the micellar nanocarriers. Furthermore, multiple dosing of RGD-PF-DP did not cause acute toxicity to the major organs of mice. Nevertheless, the acute toxicity and the long-term toxic effects of RGD-PF-DP need to be evaluated in the future. Taken together, our results suggest that the RGD-PF-DP developed in our study increased the antitumor efficacy of anticancer agents with less systemic toxicity.

Conclusion

The present study showed that RGD-PF-DP is an efficient integrin targeting DOX and PTX delivery system for the treatment of brain glioma. RGD-PF-DP displayed higher cellular uptake and stronger cytotoxicity and apoptosis induction in integrin-overexpressing U87MG cells due to c(RGDyK)-mediated endocytosis than non-c(RGDyK)-decorated Pluronic micelles. RGD-PF-DP increased the transport of the micelles across the BBB through integrin-mediated transcytosis. The anti-glioma efficacy of RGD-PF-DP was significantly enhanced compared with that of a physical mixture of DOX and PTX and PF-DP through various apoptosis pathways. Safety evaluation revealed no acute toxicity to major organs in mice after intravenous administration at treatment doses. The results of the present study indicate that RGD-PF-DP could be a promising vehicle for brain glioma therapy.

Acknowledgments

This work was supported by National Natural Science Foundation of China (81503021) and the Fundamental Research Funds for the Central Universities (22A201514055 ECUST).

Disclosure

The authors report no conflicts of interest in this work.

References

- Chen J, McKay RM, Parada LF. Malignant glioma: lessons from genomics, mouse models, and stem cells. *Cell*. 2012;149(1):36–47.
- Allard E, Passirani C, Benoit JP. Convection-enhanced delivery of nanocarriers for the treatment of brain tumors. *Biomaterials*. 2009;30(12):2302–2318.
- Stupp R, Mason WP, van den Bent MJ, et al. Radiotherapy plus concomitant and adjuvant temozolomide for glioblastoma. *N Engl J Med*. 2005;352(10):987–996.
- Liu Y, Lu W. Recent advances in brain tumor-targeted nano-drug delivery systems. *Expert Opin Drug Del*. 2013;9(6):671–686.
- Xin H, Jiang X, Gu J, et al. Angiopep-conjugated poly(ethylene glycol)-co-poly(epsilon-caprolactone) nanoparticles as dual-targeting drug delivery system for brain glioma. *Biomaterials*. 2011;32(18):4293–4305.
- Pardridge WM. BBB-Genomics: creating new openings for brain-drug targeting. *Drug Discov Today*. 2013;6(8):381–383.
- Pardridge WM. Crossing the blood-brain barrier: are we getting it right? *Drug Discov Today*. 2013;6(1):1–2.
- Pardridge WM. William Pardridge discusses the lack of BBB research. *Drug Discov Today*. 2013;7(4):223–226.
- Tao Y, Han J, Wang X, Dou H. Nano-formulation of paclitaxel by vitamin E succinate functionalized pluronic micelle for enhanced encapsulation, stability and cytotoxicity. *Colloids Surf B Biointerfaces*. 2013;102:604–610.
- Tao YH, Han JF, Ye CT, Thompson T, Dou HY. Redox-responsive gold-nanoparticle-conjugated pluronic micelle for effective anti-cancer drug delivery system. *J Mater Chem*. 2012;22(3):1864–1887.
- Saxena V, Hussain M. Formulation and in vitro evaluation of 17-allylamino-17-deoxyethoxy-22-acylamycin (17-AAG) loaded polymeric mixed micelles for glioblastoma multiforme. *Colloids Surf B Biointerfaces*. 2013;105:329–335.
- Kim JY, Choi WI, Kim YH, Tae G. Brain-targeted delivery of protein using chitosan- and RGD peptide-conjugated, pluronic-based nanocarriers. *Biomaterials*. 2012;33(4):1170–1178.
- Ma J, Wang A, Ke Z, Zheng Z. Glucose transporter and folic acid receptor-mediated Pluronic P105 polymeric micelles loaded with doxorubicin for brain tumor treating. *J Drug Target*. 2014;22(8):712–723.
- Li JY, Zhao Y, Sun MG, et al. Multifunctional liposomes loaded with paclitaxel and artemether for treatment of invasive brain glioma. *Biomaterials*. 2014;35(21):5591–5604.
- Kalish AV, Batrakova EV, Miller DW. Pluronic® block copolymers as modulators of drug efflux transporter activity in the blood-brain barrier. *Adv Drug Deliver Rev*. 2003;55:151–164.
- Miura Y, Takenaka T, Toh K, et al. Cyclic RGD-linked polymeric micelles for targeted delivery of platinum anticancer drugs to glioblastoma through the blood-brain tumor barrier. *ACS Nano*. 2013;7(10):8583–8592.
- Chen Y, Zhang W, Huang Y, Gao F, Fang X. Dual-functional c(RGDyK)-decorated Pluronic micelles designed for antiangiogenesis and the treatment of drug-resistant tumor. *Int J Nanomedicine*. 2015;10:4863–4881.
- Chen Y, Zhang W, Huang Y, Gao F, Sha X, Fang X. Pluronic-based functional polymeric mixed micelles for co-delivery of doxorubicin and paclitaxel to multidrug resistant tumor. *Int J Pharm*. 2015;488(1–2):44–58.
- Xu X, Chen X, Wang Z, Jing X. Ultrafine PEG-PLA fibers loaded with both paclitaxel and doxorubicin hydrochloride and their in vitro cytotoxicity. *Eur J Pharm Biopharm*. 2009;72(1):18–25.
- Chen Y, Sha X, Zhang W, et al. Pluronic mixed micelles overcoming methotrexate multidrug resistance: in vitro and in vivo evaluation. *Int J Nanomedicine*. 2013;8:1463–1476.
- Chen Y, Zhang W, Gu J, et al. Enhanced antitumor efficacy by methotrexate conjugated Pluronic mixed micelles against KBv multidrug resistant cancer. *Int J Pharm*. 2013;452(1–2):421–433.
- Zhang W, Shi Y, Chen Y, Ye J, Sha X, Fang X. Multifunctional Pluronic P123/F127 mixed polymeric micelles loaded with paclitaxel for the treatment of multidrug resistant tumors. *Biomaterials*. 2011;32(11):2894–2906.
- Jiang X, Xin H, Sha X, et al. PEGylated poly(trimethylene carbonate) nanoparticles loaded with paclitaxel for the treatment of advanced glioma: in vitro and in vivo evaluation. *Int J Pharm*. 2011;420(2):385–394.
- Liang B, He ML, Chan CY, et al. The use of folate-PEG-grafted-hydrated-PEI nonviral vector for the inhibition of glioma growth in the rat. *Biomaterials*. 2009;30(23–24):4014–4020.

25. Desai N. Challenges in development of nanoparticle-based therapeutics. *AAPS J*. 2012;14(2):282–295.
26. Liang YC, Su ZH, Yao Y, Zhang N. Preparation of pH sensitive Pluronic-docetaxel conjugate micelles to balance the stability and controlled release issues. *Materials*. 2015;8(2):379–391.
27. Wang YM, Lin J, Kao YT, Liu JC. Synthesis and characterization cRGD-PEG iron oxide nanoparticles of noninvasive imaging for targeting $\alpha v \beta 3$ integrins by MRI. *Proc Intl Soc Mag Reson*. 2009;17:2340.
28. Desgrosellier JS, Cheresch DA. Integrins in cancer: biological implications and therapeutic opportunities. *Nat Rev Cancer*. 2010;10(1):9–22.
29. Jiang X, Sha X, Xin H, et al. Self-aggregated pegylated poly (trimethylene carbonate) nanoparticles decorated with c(RGDyK) peptide for targeted paclitaxel delivery to integrin-rich tumors. *Biomaterials*. 2011;32(35):9457–9469.
30. Hermann DM, Bassetti CL. Implications of ATP-binding cassette transporters for brain pharmacotherapies. *Trends Pharmacol Sci*. 2007;28(3):128–134.
31. Wang J, Milner R. Fibronectin promotes brain capillary endothelial cell survival and proliferation through $\alpha 5 \beta 1$ and $\alpha v \beta 3$ integrins via MAP kinase signalling. *J Neurochem*. 2006;96(1):148–159.
32. Huang S, Li J, Han L, et al. Dual targeting effect of Angiopep-2-modified, DNA-loaded nanoparticles for glioma. *Biomaterials*. 2011;32(28):6832–6838.
33. Xin H, Chen L, Gu J, et al. Enhanced anti-glioblastoma efficacy by PTX-loaded PEGylated poly(varepsilon-caprolactone) nanoparticles: In vitro and in vivo evaluation. *Int J Pharm*. 2010;402(1–2):238–247.
34. Xin H, Sha X, Jiang X, Zhang W, Chen L, Fang X. Anti-glioblastoma efficacy and safety of paclitaxel-loading Angiopep-conjugated dual targeting PEG-PCL nanoparticles. *Biomaterials*. 2012;33(32):8167–8176.
35. Wang H, Zhao Y, Wu Y, et al. Enhanced anti-tumor efficacy by co-delivery of doxorubicin and paclitaxel with amphiphilic methoxy PEG-PLGA copolymer nanoparticles. *Biomaterials*. 2011;32(32):8281–8290.
36. Brunelle JK, Letai A. Control of mitochondrial apoptosis by the Bcl-2 family. *J Cell Sci*. 2009;122(Pt 4):437–441.
37. Du C, Fang M, Li Y, Li L, Wang X. Smac, a mitochondrial protein that promotes cytochrome c-dependent caspase activation by eliminating IAP inhibition. *Cell*. 2000;102(1):33–42.
38. Weisblum B, Haenssler E. Fluorimetric properties of the bibenzimidazole derivative hoechst 33258, a fluorescent probe specific for AT concentration in chromosomal DNA. *Chromosoma*. 1974;46(3):255–260.

International Journal of Nanomedicine

Publish your work in this journal

The International Journal of Nanomedicine is an international, peer-reviewed journal focusing on the application of nanotechnology in diagnostics, therapeutics, and drug delivery systems throughout the biomedical field. This journal is indexed on PubMed Central, MedLine, CAS, SciSearch®, Current Contents®/Clinical Medicine,

Submit your manuscript here: <http://www.dovepress.com/international-journal-of-nanomedicine-journal>

Journal Citation Reports/Science Edition, EMBase, Scopus and the Elsevier Bibliographic databases. The manuscript management system is completely online and includes a very quick and fair peer-review system, which is all easy to use. Visit <http://www.dovepress.com/testimonials.php> to read real quotes from published authors.

Dovepress